2016

Evaluation of an Extremum Seeking Control Based Optimization and Sequencing Strategy for a Chilled-water Plant

Zhongfan Zhao
University of Texas at Dallas, United States of America, zxz124130@utdallas.edu

Yaoyu Li
University of Texas at Dallas, United States of America, yxl115230@utdallas.edu

Baojie Mu
University of Texas at Dallas, United States of America, Baojie.Mu@utdallas.edu

Timothy I. Salsbury
Johnson Controls Inc., timothy.i.salsbury@jci.com

John M. House
Johnson Controls Inc., john.m.house@jci.com

Evaluation of an Extremum Seeking Control Based Optimization and Sequencing Strategy for Multiple-chiller Chilled-water Plant

Zhongfan Zhao[1]*, Yaoyu Li[2], Baojie Mu[3], Timothy I. Salsbury[4], and John M. House[5]

[1]The University of Texas at Dallas, Department of Electrical Engineering
Richardson, Texas 75080, USA
E-mail: zhongfan.zhao@utdallas.edu

[2]The University of Texas at Dallas, Department of Mechanical Engineering
Richardson, TX 75080, USA
E-mail: yaoyu.li@utdallas.edu

[3]Whirlpool, Inc.
Benton Harbor, MI 49022, USA
E-mail: sdmubaojie@gmail.com

[4] Johnson Controls, Inc., Building Efficiency Research Group
Milwaukee, WI 53201, USA
E-mail: Timothy.I.Salsbury@jci.com

[5] Johnson Controls, Inc., Building Efficiency Research Group
Milwaukee, WI 53201, USA
E-mail: John.M.House@jci.com

ABSTRACT

The ventilation and air conditioning systems of large commercial buildings are typically driven by chilled-water plants with multiple chillers. Real-time optimization and sequencing of such plants is thus critical for building efficiency (AHRI 2011). Due to the complexity and cost for calibrating chiller plant in field operation, model-free control has become an attractive solution. In an earlier study, Mu *et al*. (2015) develop an Extremum Seeking Control (ESC) based real-time optimization and sequencing strategy for a chiller-water plant with parallel chillers. Two schemes were proposed. For Scheme A, a chiller is turned on based on the measurement of chilled water valve position and is turned off when a chiller compressor is running at its nominal minimum speed. For Scheme B, a chiller is turned on and off based on the measurement of operating cooling load. Mu (2015) conducts a comprehensive simulation study on Scheme A. In this study, a comprehensive study is conducted for Scheme B under various scenarios and testing conditions, and the simulation results are compared with those from Scheme A.

1. INTRODUCTION

Currently, the ventilation and air conditioning systems of most commercial and institutional buildings are driven by chilled water plants with multiple chillers in parallel or series configuration. In order to meet the building cooling load while achieving desirable energy efficiency, the individual chillers, water pumps of the evaporating and condensing loops, and cooling tower fans are controlled with multiple control loops and sequenced based on process measurements. Considering the high power consumption of chilled-water plants, optimal control and sequencing is thus critical for energy efficiency of commercial buildings. There have been extensive literatures for optimization and sequencing of multiple-chiller plants, including rule-based control (Yu *et al*. 2008, Benton *et al*. 2002, Ahn and Mitchell 2001, Bhattacharjee 2007, Hydeman *et al*. 2002, and Qureshi and Zubair 2006), and model based control (Deng *et al*. 2014, Zhu *et al*. 2013) strategies.

Due the high dimension, nonlinear, and time-varying nature of chilled-water system plant dynamics, it is quite involved and expensive to obtain the plant models as demanded by the model based control and optimization

schemes. Therefore, model-free control and optimization approaches would be cost effective for practice. Artificial intelligence and data-driven modeling approaches have investigated (Chow *et al*. 2002, Chang *et al*. 2005, Ma and Wang 2011, Ardakani *et al*. 2008), e.g. genetic algorithm (GA), neural networks and particle swarm optimization (PSO). However, the GA and PSO approaches have inherent limitation in that they need large number of historic data or training samples for offline computation and their solutions and convergence are random.

Extremum Seeking Control (ESC) (Ariyur and Krstic 2003) has emerged as an attractive model-free real-time optimization strategy for HVAC systems (Li et al. 2010, Li et al. 2013, Dong et al. 2014, Hu et al. 2015). Recently, based on a Penalty-function based Extremum Seeking Control (ESC), Mu et al. (2015) propose a model-free real-time optimization and sequencing strategy for chilled-water plant with multiple chillers in parallel, as shown in Fig. 1, where the variable to be optimized is the total power from the chiller compressors, cooling tower fans, condenser and evaporator loop water pumps, while the manipulated inputs include the tower fan airflow, condenser water flows and evaporator leaving chilled-water temperature setpoint.

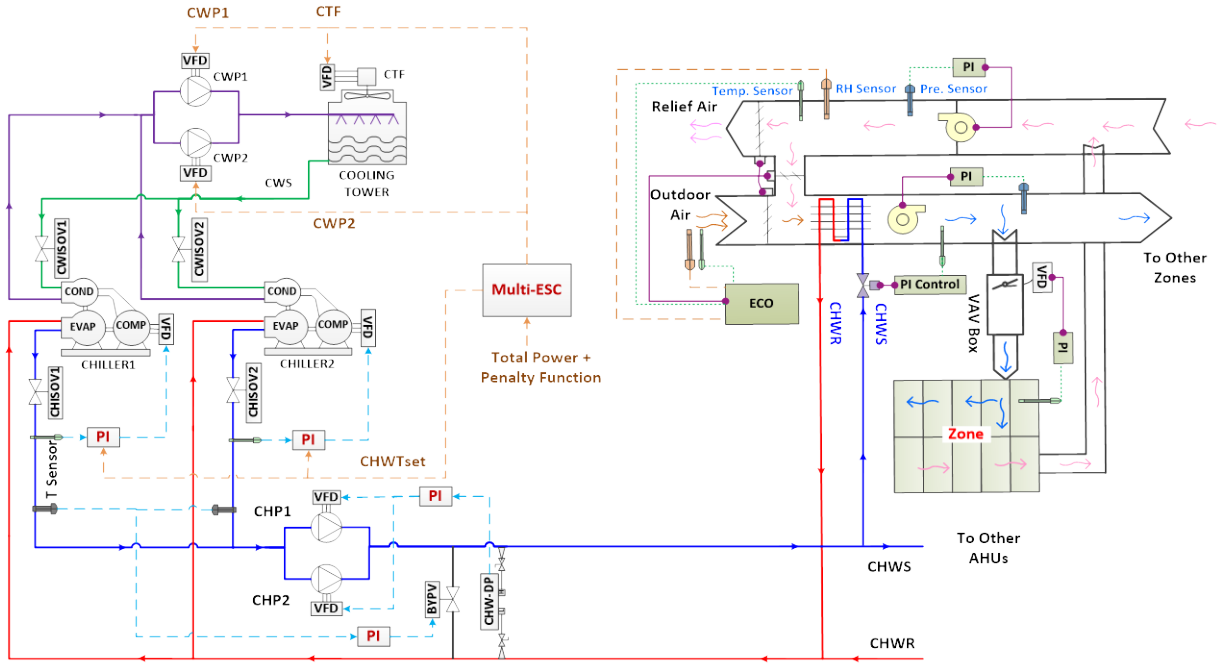

Figure 1: Schematic of a chilled-water plant with two chillers in parallel.

In particular, two schemes (Scheme A and Scheme B) are proposed for chiller sequencing. For Scheme A, a chiller is turned on based on the measurement of chilled water valve position and is turned off when a chiller compressor is running at its nominal minimum speed. For Scheme B, a chiller is turned on and off based on the measurement of operating cooling load. For Scheme A, Mu (2015) performed comprehensive case studies, and the simulation results have well justified the performance of the proposed framework under various ambient, load and equipment conditions. However, for Scheme B, only one scenario is simulated for idea proof purpose. Although the two chiller sequencing schemes have shared physical ground in terms of chiller plant operation, the load based Scheme B will be more appropriate for field implementation.

The objective of this study is to conduct comprehensive study on the performance of Scheme B based optimization and sequencing strategy for various ambient and load conditions. The remainder of this paper is structured as follows. Section 2 presents the details of Scheme A and Scheme B, and the simulation results are given in Section 3. The paper is concluded in Section 4, along with the plan for future work.

2. ESC BASED OPTIMAL CONTROL AND SEQUENCING FOR CHILLED-WATER PLANT WITH PARALLEL CHILLERS

The schematic of a chilled-water plant with *N* chillers in parallel is shown in Figure 2. Each chiller has its own compressor (COMP) regulating the evaporator leaving chilled water temperature (CHWT), a condenser water pump (CWP) adjusting the condenser water flow rate (CWF), and a chilled water pump (CHP) adjusting the supplying

chilled water flow rate (CHF) to the cooling coils of the air-handling unit (AHU). As a simplified treatment, the condensing water from all chillers is assumed to share one cooling tower, and the cooling-tower air (CTA) flow is adjusted by a cooling tower fan (CTF).

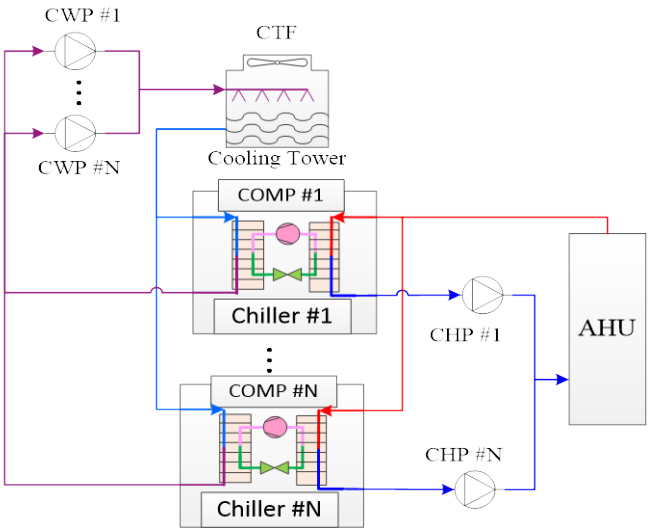

Figure 2: A chilled-water plant with *N* chillers in parallel.

Chiller plant optimization aims to minimize the total power consumption, provided that regulation of the AHU supply air temperature (SAT) is satisfactory and the suction superheat for the compressors of all operating chillers. The associated ESC aims to find the optimum input u such that

$$u^*(t) = \arg\min_u P_t(t) = \arg\min_u \left\{ P_{CTA}(t) + \sum_{i=1}^{n} \delta_i \left[P_{COMP,i}(t) + P_{CWF,i}(t) + P_{CHF,i}(t) \right] \right\} \tag{1}$$

with $u \triangleq [\dot{m}_{CTA}, \dot{m}_{CWF,1}, \dot{m}_{CHF,1}, T_{set,1}, \cdots, \dot{m}_{CWF,n}, \dot{m}_{CHF,n}, T_{set,n}]$, and the following constraints imposed:

$$\dot{m}_{CTA,\min} \le \dot{m}_{CTA} \le \dot{m}_{CTA,max} \tag{2}$$

$$\dot{m}_{CWF,i,\min} \le \dot{m}_{CWF,i} \le \dot{m}_{CWF,i,max} \tag{3}$$

$$\dot{m}_{CHF,i,\min} \le \dot{m}_{CHF,i} \le \dot{m}_{CHF,i,max} \tag{4}$$

$$\Omega_{COMP,i,min} \le \Omega_{COMP,i} \le \Omega_{COMP,i,max} \tag{5}$$

$$T_{SH,i,\min} \le T_{SH,i} \le T_{SH,i,max} \tag{6}$$

with binary variables δ_i indicating ON or OFF operation for chiller *i* with value of 1 or 0. The controls inputs for ESC based chiller sequencing for a chilled-water plant with multiple chillers in parallel are selected as: cooling tower air flow rate, condenser water flow rate and leaving chilled water temperature of each chiller. As a simplified treatment, all chillers are assumed to have the same CHWT setpoint. To handle the constraints of plant inputs, the objective function is augmented with a penalty term in addition to the total power consumption, i.e. , $L_p(t) = P_t(t) + y_p(t)$ with respect to the regulation of $\dot{m}_{CTA}, \dot{m}_{CWF}$, and T_{set}, where T_{set} is the CHWT setpoint regulated by the compressor speed. $y_p(t)$ is the penalty function defined as:

$$\begin{aligned} y_p(t) = \sum_{i=1}^{n} \phi_i(\cdot) = & \frac{1}{2}\gamma_{CTA}(\dot{m}_{CTA} - \dot{m}_{CTA,sat})^2 + \frac{1}{2}\gamma_{CWF,i}(\dot{m}_{CWF,i} - \dot{m}_{CWF,i,sat})^2 + \frac{1}{2}\gamma_{COMP,i}(\Omega_{COMP,i} - \Omega_{COMP,i,sat})^2 \\ & + \frac{1}{2}\gamma_{CHF,i}(\dot{m}_{CHF,i} - \dot{m}_{CHF,i,sat})^2 + \frac{1}{2}\gamma_{SH,i}(T_{SH,i} - T_{SH,i,sat})^2 \end{aligned} \tag{7}$$

Subscript '*sat*' refers to the output of the limiter. In Eq. (9), parameters $\gamma_{CWF,i}$, γ_{COMP}, $\gamma_{CHF,i}$, $\gamma_{SH,i}$ and γ_{CTA} are weights of penalty terms for the saturation of $\dot{m}_{CWF,i}$, $\Omega_{COMP,i}$, $\dot{m}_{CHF,i}$, $T_{SH,i}$ and $\dot{m}_{CTA}$, respectively.

2.1 Scheme B for Chiller Sequencing

i) Turn on/off a chiller

The $(n+1)^{\text{-th}}$ chiller is turned on (i.e. $\delta_{n+1}=1$) if $\dot{Q}(t) > \sum_{i=1}^{n+1} \dot{Q}_{i,\min}$ for $t \in [t_0, t_0+\tau]$, where the chiller load is calculated by $\dot{Q} = c_p \dot{m}(T_r - T_s)$ based on the temperature measurements of the supply water and return water, and the supply water mass flow rates for all operating chillers. $\dot{Q}_{i,\min}$ is the nominal minimum chiller capacity for Chiller *i* based on manufacturer's specification or historical calibration data. Similarly, the $(n+1)^{\text{-th}}$ chiller is turned off (i.e. $\delta_{n+1}=0$) if $\dot{Q}(t) \le \sum_{i=1}^{n+1} \dot{Q}_{i,\min}$, for $t \in [t_0, t_0+\tau]$.

ii) Chiller startup and shutdown.

To turn on the $i^{\text{-th}}$ chiller, the chiller compressor speed is first increased from zero to the nominal minimum speed $\Omega_{COMP,i,\min}$ following a specific (startup) ramp. Then, the compressor speed is used to regulate the evaporator leaving chilled water temperature (CHWT) at its setpoint. Meanwhile, chilled water pump (CHP) is started from zero flow to the nominal minimum flow during the startup period following a specific ramp, and then the chilled water valve is used to regulate the AHU supply air temperature (SAT) setpoint. The condenser water flow rate (CWP) is started from zero flow to the pre-set value during the startup period following a specific ramp. To turn off a chiller, the chiller compressor speed is first disconnected from the CHWT control loop, and then decreased from the current speed to 0 following a specific (shutdown) ramp. Meanwhile, the CHP is slowed from its current speed to zero flow during shutdown. The CWP's are turned off to 0 from its previous values during shutdown.

iii) Enable/Disable ESC

Assume *n* chillers are in operation. During the startup period of the $(n+1)^{\text{-th}}$ chiller, the ESC for *CH*1 through *CHn* and the cooling tower is disabled, and corresponding ESC control inputs are frozen to their current values, while the condenser water flow rate of the $(n+1)^{\text{-th}}$ chiller will become a new control input for the ESC that includes CH1 through CH(n+1) and the cooling tower. After the startup process, the ESC with increased input dimension is started.

Assume $(n+1)$ chillers are on, and the $(n+1)^{\text{-th}}$ chiller is to be shut down. The ESC for *CH*1 through *CHn* and cooling tower is disabled by freezing the control inputs to their current values, while the control inputs of condenser water flow rate (CWF) and the CHWT setpoint for the $(n+1)^{\text{-th}}$ chiller are frozen and disabled. After shutdown of the $(n+1)^{\text{-th}}$ chiller, the ESC for *CH*1 through *CHn* and cooling tower resumes its action, and the initial values of control inputs are the previously frozen values, while the control inputs for the $(n+1)^{\text{-th}}$ remain disabled until conditions in 1) are satisfied.

iv) Bumpless transfer between chiller startup/shutdown and ESC.

To achieve bumpless transfer between the chiller startup/ shutdown operation and the ESC, the conditional integration (CI) scheme (Peng *et al*. 1993) is adopted, see Mu et al. (2015) for details . The CI scheme switches the input of the integrator to zero, and disables the modulation and demodulation signals when ESC is disabled during the chiller startup/shutdown operation. Similarly, the CI scheme switches the input of the integrator to the output of LP filter, and enables the modulation and demodulation signals when ESC is engaged.

3. SIMULATION RESULTS

In order to give a comprehensive evaluation of Scheme B for ESC based chiller sequencing control, simulations are performed for the scenarios defined in Table 1. Three ambient conditions are considered: i) 27°C and 60 % RH ("Mild"), ii) 37°C and 30 %RH ("Dry Hot"), and iii) 37°C and 80 %RH ("Humid Hot"). For each of these ambient conditions, simulation analysis are made in Scenario#1, 2, 5, 6. Scenario#3 is simulated with dynamic ambient and load profiles. The simulations are carried out with the Modelica based dynamic simulation model for a variable primary flow (VPF) chilled-water plant developed by Mu (2015), which has two parallel chillers, one cooling tower, an AHU including a VAV box and a single zone.

Table 1: Simulation scenarios for each ambient condition

Scenario #	Description
1	Two-chiller ESC with no sequencing under fixed ambient conditions

2	Chiller sequencing under variable load and fixed ambient conditions
3	Chiller sequencing with realistic ambient and load profile
4	Penalty Function based ESC Chiller Sequencing
5	ESC for Efficiency Recovery: Chiller A properly charged and Chiller B with a low charge
6	ESC for Efficiency Recovery: Chiller A nominal + Chiller B with heat exchanger fouling

3.1 Simulation Case#1

The multivariate ESC is tested with two chillers in parallel with the fixed ambient conditions and fixed load. The internal heat gain is chosen as 350 kW. Table 2 gives the ESC design parameters. Fig. 3 shows the ESC inputs and out trajectories for the three ambient conditions. For all cases, the cooling tower air flow rate and chilled water leaving temperature start at 23kg/s and 8°C. The initial value of condenser water flow rate for both chillers are 25kg/s. The power consumption of the chilled-water plant are 217.4kW, 302.4kW and 335.9kW respectively. They decrease 12.4%, 6.4% and 6.1%. The superheat, supply-air temperature and zone temperature are well regulated about their respective setpoint of 5°C, 13°C and 25°C.

Table 2: ESC controller parameters for two chiller without sequencing

Parameter	**ESC1**	**ESC2**	**ESC3**	**ESC4**
Dither Freq.(rad/s)	0.005	0.0038	0.0013	0.0023
Dither Amp.	3 kg/s	3 kg/s	0.5℃	3 kg/s
Demodulation Amp.	2/3 kg/s	2/3 kg/s	4 ℃	2/3 kg/s
Demodulation Phase (rad)	0.15	0.1	0.18	0.05
ω_{BPL} (rad/s)	0.0045	0.0034	0.0012	0.0021
ω_{BPH} (rad/s)	0.0055	0.0042	0.0014	0.0025
ω_{LP} (rad/s)	0.005/3	0.0038	0.0013	0.0023
Integrator Gain	0.0006	0.0006	0.000011	0.0006
Input range	[5, 60]kg/s	[5, 30]kg/s	[1, 11]℃	[5, 30]kg/s

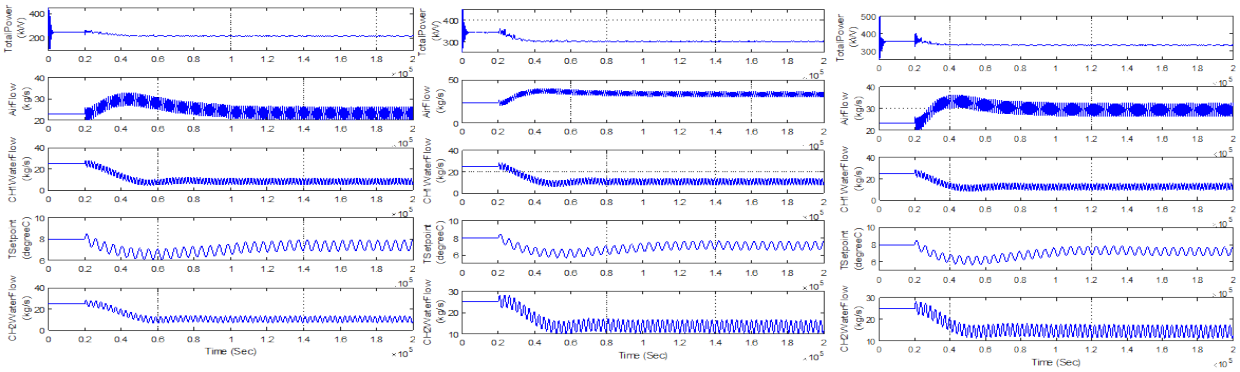

Figure 3: Scenario 1 under mild, dry-hot and humid-hot ambient conditions (from left to right)

3.2 Simulation Case#2

This case is based on two chillers working in parallel with the fixed ambient conditions and variable internal heat load. Scheme B-based optimization and sequencing strategy is applied in this scenario. The ambient conditions are the same with case#1. In the "Mild" condition, the internal heat gain experience a ramp change at 108000 sec (30 hr) from 180 kW to 300 kW with period of 3600 sec, and a 3600-second ramp change at 219600 sec (61 hr) from 300 kW to 180 kW, respectively. In the "Humid Hot" condition, the internal heat gain experience a ramp change at 108000 sec (30 hr) from 150 kW to 250 kW with period of 3600 sec, and a 3600-second ramp change at 219600 sec (61 hr) from 250 kW back to 150 kW, respectively. And in the "Dry Hot" condition, the internal heat gain experience a ramp change at 108000 sec (30 hr) from 180 kW to 300 kW with period of 3600 sec, and a 3600-second ramp change at 219600 sec (61 hr) from 300 kW back to 180 kW, respectively. The ESC controller parameters are summarized in Table 3.

Table 3: ESC controller parameters for two chiller with sequencing

Parameter	ESC1	ESC2	ESC3	ESC4
Dither Freq.(rad/s)	0.005	0.0038	0.002	0.0023
Dither Amp.	3 kg/s	3 kg/s	0.5°C	3 kg/s
Demodulation Amp.	2/3 kg/s	2/3 kg/s	4 °C	2/3 kg/s
Demodulation Phase (rad)	0.15	0.1	0.18	0.05
ω_{BPL} (rad/s)	0.0045	0.0034	0.0018	0.0021
ω_{BPH} (rad/s)	0.0055	0.0042	0.0022	0.0025
ω_{LP} (rad/s)	0.005/3	0.0038	0.002	0.0023
Integrator Gain	0.00072	0.00048	0.000033	0.000288
Input range	[5, 60]kg/s	[0.5, 30]kg/s	[1, 11] °C	[0.5, 30]kg/s

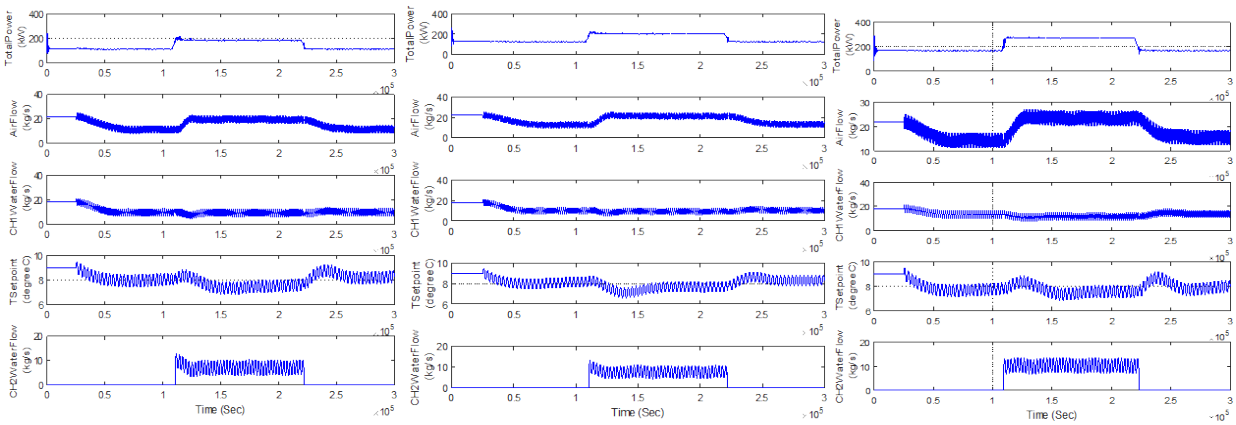

Figure 4: Scenario 2 under mild, dry-hot and humid-hot ambient conditions (from left to right).

In this scenario, the four-input ESC has its input and output trajectories shown in Fig. 4, which also represent the simulation results under three different ambient conditions ('Mild', 'Dry hot' and 'Humid hot') respectively. Under these three ambient conditions, the initial cooling tower air flow rate, chilled water leaving temperature setpoint and condenser water flow rate are 22 kg/s, 9°C and 18 kg/s. The three-input ESC for chiller 1 is turned on at 20000 sec. The ESC search results in an average steady-state total power of 115.1 kW, 124.5 kW and 164.5 kW under the load of 180 kW, 180 kW and 150 kW respectively. The optimal cooling tower air flow rate are 11.5 kg/s, 12.4 kg/s and 14.5 kg/s, chiller 1 condenser water flow rate are 9.8 kg/s, 10.3 kg/s and 12.9 kg/s, and leaving chilled-water temperature setpoint are 8.1°C, 8.0°C and 7.7°C.

With the load increasing, chiller 2 is engaged at around 110000 sec for all three ambient conditions. The four-input ESC reach an average steady-state total power of 184.5 kW, 204.6 kW and 268.1 kW under the load of 300 kW, 300 kW and 250 kW respectively. The optimal cooling tower air flow rate are 19.8 kg/s, 21.2 kg/s and 23.7 kg/s, chiller 1 condenser water flow rate are 9.4 kg/s, 9.7 kg/s and 12.0 kg/s, chiller 2 condenser water flow rate are 7.2 kg/s, 7.8 kg/s and 9.8 kg/s, and leaving chilled-water temperature setpoint are 7.5°C, 7.6°C and 7.4°C. With the load decreasing back to the previous value, chiller 2 is turned off at about 220000 sec. The three-input ESC's average steady-state total power, optimal cooling tower air flow rate, chiller 1 condenser water flow rate and leaving chilled-water temperature setpoint are all back to the previous values.

The gradient trajectories are plotted in second subplot of Fig. 7, 8, 9 to examine the convergence of each ESC channel. The oscillation of gradients of each channel about 0 at steady state indicates that the ESC has converged to an interior optimum. Similar with Case#1, other subplots show that the superheat, supply-air temperature and zone temperature are well regulated about their respective setpoint of 5°C, 13°C and 25°C.

3.3 Simulation Case#3

Case#3 relies on a 32-hr ambient temperature and RH profile developed from the TMY2 data for the Dallas-Fort Worth area (National Solar Radiation Data Base) and a variable load file is also used. Scheme B-based sequencing control is also applied in this scenario. Table 4 shows the ESC controller parameters in this case. The initial condition is set as: cooling tower air flow rate of 22 kg/s, chiller 1 and chiller 2 condenser water flow rate of 18 kg/s,

and leaving chilled-water temperature setpoint of 9°C. As shown in Fig. 5, the ESC is turned on at t = 7 hr. In response to the variation of ambient condition and internal cooling load, chiller 2 is turned on at t=20.3 hr.

Table 4: ESC controller parameters for two chiller with realistic ambient and load profile

Parameter	ESC1	ESC2	ESC3	ESC4
Dither Freq.(rad/s)	0.005	0.0038	0.002	0.0023
Dither Amp.	3 kg/s	3 kg/s	0.5°C	3 kg/s
Demodulation Amp.	2/3 kg/s	2/3 kg/s	4°C	2/3 kg/s
Demodulation Phase (rad)	0.15	0.1	0.18	0.05
ω_{BPL} (rad/s)	0.0045	0.0034	0.0018	0.0021
ω_{BPH} (rad/s)	0.0055	0.0042	0.0022	0.0025
ω_{LP} (rad/s)	0.005/3	0.0038	0.002	0.0023
Integrator Gain	0.00096	0.00048	0.000033	0.000288
Input range	[5, 60]kg/s	[0.5, 35]kg/s	[1, 11] °C	[0.5, 35]kg/s

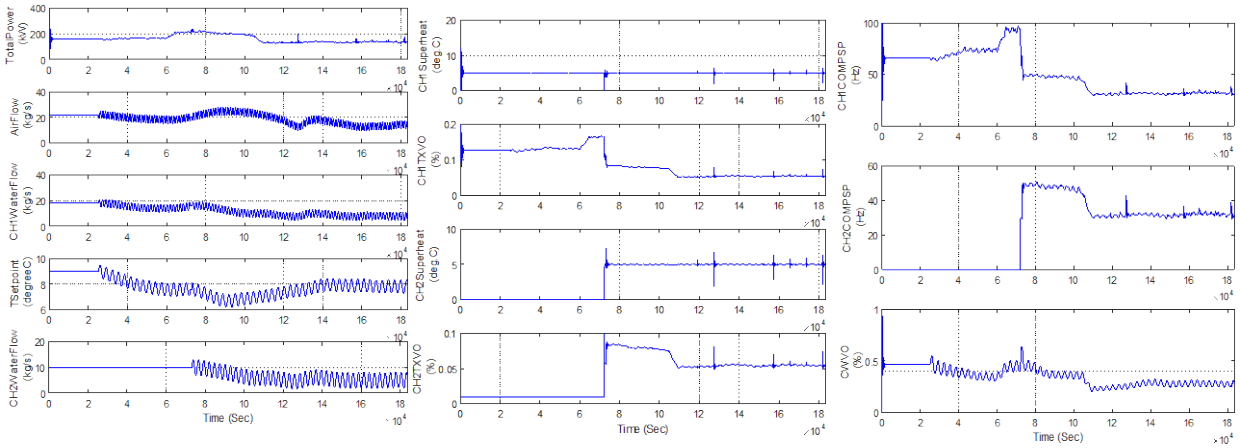

Figure 5: Scenario 3 under realistic ambient condition

3.4 Simulation Case#4

In order to study the input saturation impact on ESC-based chiller sequencing control, the cooling tower air flow was limited to 25 kg/s. The ambient conditions is 37°C and 30 %RH. The internal cooling load follows a 28000s positive ramp at t = 80000s from 250 kW to 400 kW, and a 1-hr negative ramp at t =219600s from 400 kW to 150 kW, respectively. The ESC controller parameters are the same as Case#3. The simulation results are shown in Fig. 6. The ESC feedback is the sum of the total power and penalty terms when input saturation occurs. The weight of penalty term for cooling tower air flow channel is γ_{CTA} = 1.1.

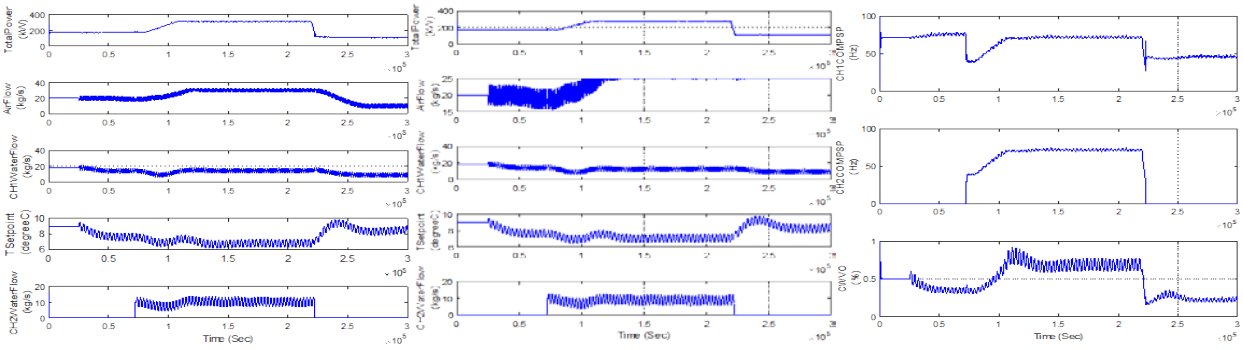

Figure 6: Scenario 4 under dry hot ambient condition

On average, ESC results in cooling tower air flow rate of 19.3 kg/s, chiller 1 condenser water flow rate of 14.1 kg/s, leaving chilled-water temperature setpoint of 6.9°C under the 250 kW load. With the load increased to 400 kW, chiller 2 is engaged and the cooling tower air flow rate is saturated at its upper limit of 25 kg/s while the chiller 1

condenser water flow settles to 14.4 kg/s, the leaving chilled-water temperature setpoint converges to 6.7°C, the chiller 2 condenser water flow rate converges to 10.2 kg/s, respectively. When the load goes down to 150 kW after 31 hour, the ESC converges to the cooling tower air flow rate of 10.5 kg/s, the chiller 1 condenser water flow rate of 8.3 kg/s, and leaving chilled-water temperature setpoint of 8.6°C. The standard ESC without a penalty function get its saturated input stuck at the saturate value regardless of the external condition changing.

3.5 Simulation Case#5

In practice, a major cause for suboptimal operation of HVAC systems is equipment degradation. For chiller plants, equipment degradations may include heat exchanger fouling, low refrigerant charge, cooling tower fill deposits, and compressor wear. In this case, low refrigerant situation is discussed. Chiller 2 properly charged and Chiller 1 with a 40% refrigerant charge. And the ambient conditions and load are the same as Case#1. The design parameters of this four-input ESC are also the same as Case#1.

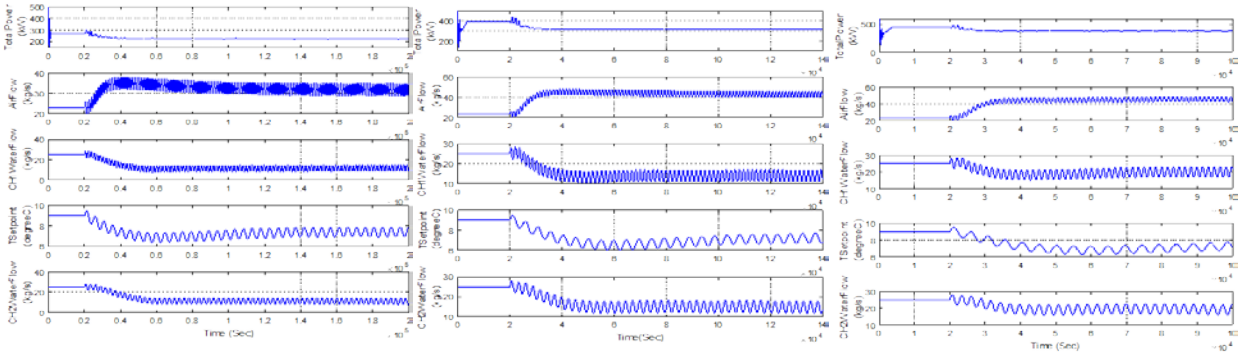

Figure 7: Scenario 5 under dry hot, mild and humid-hot ambient conditions (from left to right).

The average steady-state total power under three different ambient conditions ('Mild', 'Dry hot' and 'Humid hot') are 228.2 kW, 318.5 kW and 381.5 kW respectively shown in Fig. 7. They decrease 16.9%, 18.8% and 14.7%.respectively. Under all three ambient condition, the cooling tower air flow rate, condenser water flow rate for both chillers and chilled water leaving temperature setpoint start at 23kg/s, 25kg/s and 9°C. The four-input ESC converges to the cooling tower air flow rate of 32.5 kg/s, 43.2 kg/s and 45.3 kg/s respectively, the chiller 1 condenser water flow rate of 12.2 kg/s, 13.6 kg/s and 19.7 kg/s respectively, chiller 2 condenser water flow rate of 11.0 kg/s, 14.9 kg/s and 19.7 kg/s respectively and leaving chilled-water temperature setpoint of 7.5°C, 7.3°C and 6.9°C respectively. The superheat, supply-air temperature and zone temperature are well regulated about their respective setpoint of 5°C, 13°C and 25°C. Since the ambient condition and load are the same as Case#1(both chillers are fully charged), the overall power consumption increase with a low refrigerant-charged chiller.

3.6 Simulation Case#6

In this case, another equipment degradation situation for chiller plants is considered. Chiller 2 with nominal operation and Chiller 1 with heat exchanger (HX) fouling. The overall effect of HX fouling is modeled by a fouling factor R_f (Ardakani *et al*. 2008, Mu 2015), Chiller 1 evaporator is set as $R_f = 0.0001$ and the chiller 1 condenser is set as $R_f = 0.00025$. The simulation runs with the same ambient condition, load and ESC parameters as Case#1. The ESC search result in an average steady-state total power under three different ambient conditions ('Mild', 'Dry hot' and 'Humid hot') are 220.6 kW, 310 kW and 345.4 kW respectively, i.e. resulting in decrease of 13.8%, 11.9% and 7.6%, respectively. For all three ambient conditions, the cooling tower air flow rate and chilled water leaving temperature start at 23kg/s and 8°C. The initial value of condenser water flow rate for both chillers are 25kg/s. The four-input ESC converges to the cooling tower air flow rate of 23.5 kg/s, 33.5 kg/s and 30.8 kg/s respectively, the chiller 1 condenser water flow rate of 8.4 kg/s, 11.2 kg/s and 12.27 kg/s respectively, chiller 2 condenser water flow rate of 10.6 kg/s, 13.6 kg/s and 15.5 kg/s respectively and leaving chilled-water temperature setpoint of 7.4°C, 7.1°C and 7.2°C respectively. Moreover, the superheat, supply-air temperature and zone temperature are well regulated about their respective setpoint of 5°C, 13°C and 25°C. Compared with no system degrades Case#1, the total power consumption increase in this case, whileas ESC still can track the optimal input setting for the maximum achievable efficiency when the system degrades with HX fouling under various ambient conditions.

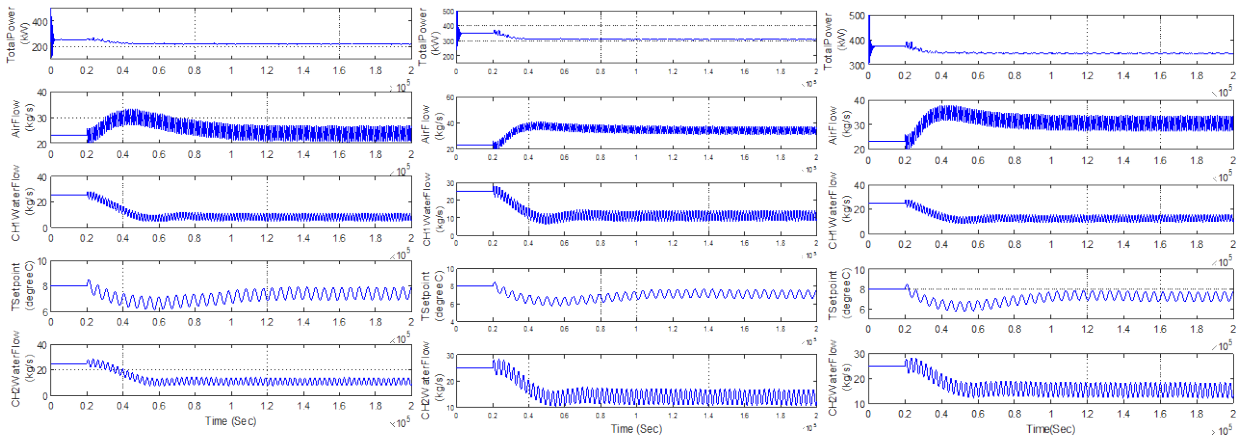

Figure 8: Scenario 6 under mild, dry-hot and humid-hot ambient conditions (from left to right).

3.7 Simulation results comparison of Scheme A and Scheme B

Scheme A and Scheme B are compared with Case #3 of Mu (2015) under the "Mild" condition, for which the internal heat gain experienced a 30000-sec ramp change at 200,000s from 250kW to 500kW, and a ramp change at 350,000 sec from 500kW to 200kW also with a 30000-sec ramp, respectively. The simulation results are shown in Fig. 9. Both Scheme A and Scheme B can activate and deactivate the additional chiller according to the criterion respectively. Since the load varies, the whole simulation process is divided into three periods. In the period 1 (0 to 2×10^5 s) and period 3 (3.8×10^5 to 5.76×10^5 s), only chiller 1 works and in period 2 (2.3×10^5 to 3.5×10^5 s), both chillers are engaged due to the heavy load. The ESC channels comparison of Scheme A and Scheme B is listed in Table 5. During period 2 and period 3, Scheme B achieves better performance, since it has less power consumption. However, during period 1, Scheme A has better efficiency. Moreover, the chiller 2 is turned on 6000s earlier and turned off 13400s earlier when Scheme B is applied.

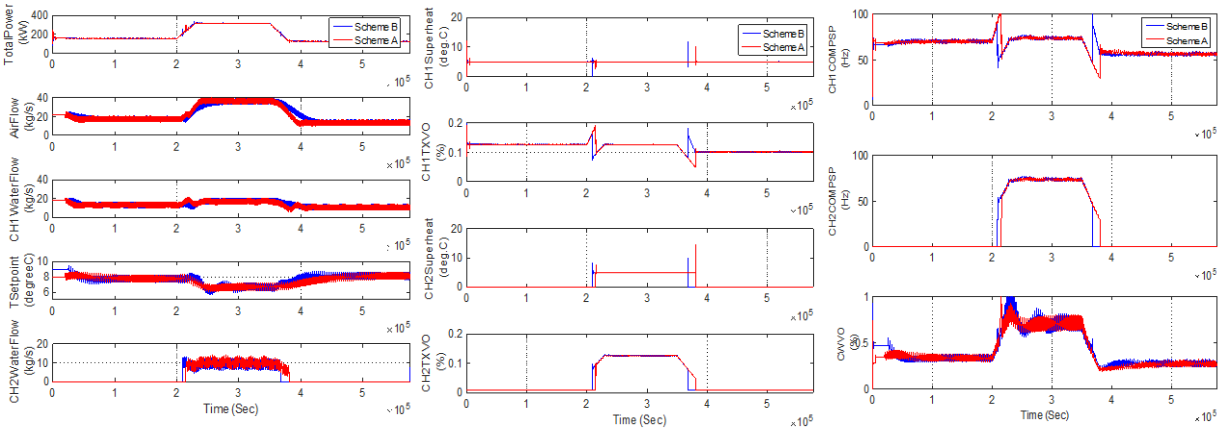

Figure 9: Scheme B and Scheme A under the same external condition

Table 5: ESC channels comparison of Scheme A and Scheme B

	Scheme A			Scheme B		
	Period 1	Period 2	Period 3	Period 1	Period 2	Period 3
Total power (kW)	156.9	316.2	126.3	158.9	315.3	125.7
Air flow (kg/s)	17.2	36.7	13.5	17.6	36.4	13.3
Chiller 1 water flow (kg/s)	13.2	16.7	10.5	13.4	17.4	10.9
Tsetpoint (°C)	7.6	6.6	7.9	7.7	6.7	8.1
Chiller 2 water flow (kg/s)	0	10.1	0	0	9.2	0

4. CONCLUSIONS AND FUTURE WORK

A multivariate ESC based chiller sequencing control algorithm is studied in this paper. It maximizes the chilled water plant energy efficiency in real time under different external conditions. Based on a dynamic chilled water plant simulation model with two chillers in parallel, several scenarios are discussed in order to evaluate the performance of the proposed ESC algorithm. The simulation results show that significant energy saving is obtained and the effectiveness of the proposed Scheme B based chiller sequencing is also validated in various conditions. By comparing the performance of Scheme A and B under the same external condition, the overall power consumption is quite similar. More detailed study is under way.

REFERENCES

AHRI Standard 550/590 (I-P), 2011 Standard for Performance Rating of Water-Chilling and Heat Pump Water-Heating Packages using the Vapor Compressor Cycle, Air-Conditioning, Heating & Refrigeration Institute, 2011.

Ardakani, A.J., Ardakani, F.F., and Hosseinian, S.H. (2008), "A Novel Approach for Optimal Chiller Loading Using Particle Swarm Optimization. Energy and Buildings", 40 (12), pp. 2177-2187.

Mu, B., Li, Y.and Seem, J.E. (2014) "Experimental Study on Extremum Seeking Control for Efficient Operation of Airside Economizer", 2014 Purdue Compressor Engr., Refri. & Air Cond., and High Perf. Bldgs. Conf., 10 pages.

Mu, B., Li, Y., Salsbury, T.I., House, J.M. (2015) "Extremum Seeking Based Control Strategy for a Chilled-Water Plant with Parallel Chillers," ASME Dynamic Systems and Control Conf., Columbus, OH, Paper #9949, 10 pages.

Mu, B, (2015) "Self-optimizing Control for Building Ventilation and Air Conditioning Systems", Ph.D. Dissertation, Department of Electrical Engineering, University of Texas at Dallas, December 2015.

National Solar Radiation Data Base, 1961-1990: Typical Meteorological Year 2, http://rredc.nrel.gov/solar/old_data/nsrdb/1961-1990/tmy2/.

Yu, F.W., Chan, K.T., 2008, "Optimization of water-cooled chiller system with load-based speed control," *Applied Energy*, **85** (10), pp. 931-950.

Benton, D.J., Hydeman, M., Bowman, C.F., Miller, P., 2002, "An Improved Cooling Tower Algorithm for The CoolTools™ Simulation Model," *ASHRAE Transactions*, **108**(1), Paper No. AC-02-9-4.

Hydeman, M., Zhou, G., 2007, "Optimizing chilled water plant control," *ASHRAE Journal*, pp. 45-54.

Ahn, B.C., Mitchell, J.W., 2001, "Optimal control development for chilled water plants using a quadratic representation", *Energy and Buildings*, **33**, pp. 371-378

Bhattacharjee K. 2007, "Reducing energy cost in an industrial chilled water plant", *Energy Engr.*, **107**(4): 42–51.

Hydeman, M., Webb, N., Sreedharan, P., Blanc, S., 2002, "Development and testing of a reformulated regression based electric chiller model," *ASHRAE Transactions* 108(2), pp. 1118 – 27.

Qureshi B., Zubair S. 2006, "Prediction of evaporation losses in wet cooling towers," *Heat Tsfr. Engr.*, **27**(9):86–92.

Deng, K., et al., 2014, "Model predictive control of central chiller plant with thermal energy storage via dynamic programming and mixed- integer linear programming," *IEEE Trans. Auto. Sci. & Eng*. pp. 1-14.

Zhu, J., Yang, Q., Lu, J., 2013, "Model predictive control of chilled water temperature for centrialized HVAC systems", *2013 IEEE Electrical Power & Energy Conference*, 5 pages.

Chow, T.T., Zhang, G.Q., Lin, Z., Song, C.L., 2002, "Global optimization of absorption chiller system by genetic algorithm and neural network," *Energy and Buildings*, 34 (1), pp. 103-109.

Chang, Y.-C., Lin, J.-K., and Chuang, M.-H., 2005, "Optimal chiller loading by genetic algorithm for reducing energy consumption," *Energy and Buildings*, 37 (2), pp. 147-155.

Ma, Z., and Wang, S. 2011, "Supervisory and optimal control of central chiller plants using simplified adaptive models and genetic algorithm," *Applied Energy*, 88 (1), pp. 198-211.

Li, P., Li, Y., and Seem, J.E., 2010, "Efficient Operation of Air-Side Economizer Using Extremum Seeking Control," *ASME J. Dyn. Sys., Meas. & Control*, 132(3): 031009 (10 pages).

Li, X., Li, Y., and Seem, J.E., 2013, "Dynamic Modeling and Self-Optimizing Operation of Chilled Water Systems Using Extremum Seeking Control", *Energy and Buildings*, **58**, pp. 172-182.

Dong, L., Li, Y., Mu, B., Xiao, Y., 2014, "Self-optimizing control of air-source heat pump with multivariable extremum seeking", *Applied Thermal Engineering*, **84**(5), pp. 180-195.

Hu, B., Li, Y., Cao, F. and Xing, Z. "Extremum Seeking Control of COP Optimization for Air-Source Transcritical CO2 Heat Pump Water Heater System," *Applied Energy*, Vol. 147, pp. 361-372, June 2015.

Peng, Y., Vrancic, D., Hanus, R., 1993. "Anti-windup, bumpless and conditioned transfer techniques for PID controllers", *IEEE Trans. Control Sys. Tech.*, **16**(4), pp. 48-57.